5

Application of meta-material concepts

Ho-Yong Kim[1] and Hong-Min Lee[2]
[1]*ACE antenna,*
[2]*Kyonggi University*
Korea

1. Introduction

Wave propagation in suppositional material was first analyzed by Victor Vesalago in 1968. Suppositional material is characterised by negative permittivity and negative permeability material properties. Under these conditions, phase velocity propagates in opposite direction to group velocity. This phenomenon is referred to as "backward wave" propagation. The realization of backward wave propagation using SRR (Split Ring Resonator) and TW (Thin Wire) was considered by Pendry in 2000. Since then, these electrical structures have been studied extensively and are referred to as meta-material structures. In this chapter we will analyze meta-material concepts using transmission line theory proposed by Caloz and Itho and propose effective materials for realising these concepts. We propose a novel NPLH (Near Pure Left Handed) transmission line concept to reduce RH (Right Handed) characteristics and realize compact small antenna designs using meta-material concepts. In addition we consider enhancing radiation pattern gain of an antenna using FSS (Frequency Selective Surface) and AMC (Artificial Magnetic Conductor). Finally the possibility of realising negative permittivity using EM shielding of concrete block is considered.

2. Means of meta-material concepts

The RH and LH transmission lines are shown in Fig. 1.

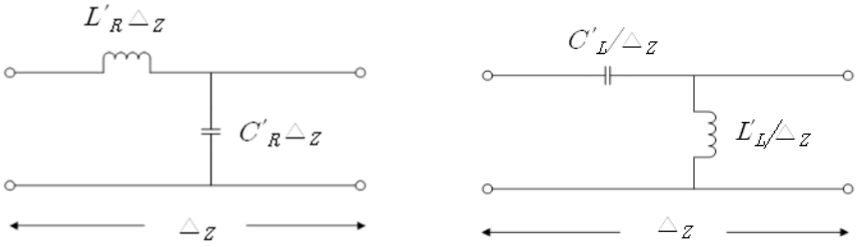

(a) RH transmission line (b) LH transmission line

Fig. 1. RH and LH transmission lines

The RH (Right Handed) transmission line consists of serial inductance($L_R^{'}$) and parallel capacitance ($C_R^{'}$). The serial inductance ($L_R^{'}\Delta z$) and prallel capacitance ($C_R^{'}\Delta z$) per unit lenth are as following equatiion.

$$C_R'\Delta z = \varepsilon_0\varepsilon_r\frac{w}{d}(F/m) \qquad L_R'\Delta z = \mu_0\mu_r\frac{d}{w}(H/m) \tag{1}$$

Where, the w is width of transmission line, the d is thickness of substrate.

We will consider negative permittivity and negative permeability in transmission line. The serial inductance ($L_R^{'}\Delta z$) and parallel capacitance (B_{meta}) are replaced as negative reactance(X_{meta}), which are expressed as following equation.

$$X_{meta}\text{=-j}\omega|L_R'\Delta z| = -j\frac{1}{\omega C_{eff}} \qquad B_{meta}\text{=-j}\omega|C_R'\Delta z| = -j\frac{1}{\omega L_{eff}} \tag{2}$$

We know that electrical performance of L_R' and C_R' are changed into serial capacitance(C_L') and prallel inductance(L_L') in negative permeability and negative permittivity material.
If we added serial capacitance on normal transmission line, the transmission line with serial capacitance exhibits similar transmission line characteristic using ENG (Epsilon Negative) material. Also, if we use parallel inductance on normal transmission line, the transmission line with parallel inductance express transmission line using MNG (Mu Negative) material. Therefore, we know that the metamaterial concepts can be realized by electrical loading structures, which are gap of microstrip line, via and so on.
The applications of meta-material are shown in Fig. 2. The SNG (Single Negative) materials include ENG material and MNG material. The DNG (Double Negative) material has negative permittivity and negative permeability simultaneously. We will deal with small antenna, CRLH (Composite Right/Left Handed) transmission line, FSS and AMC

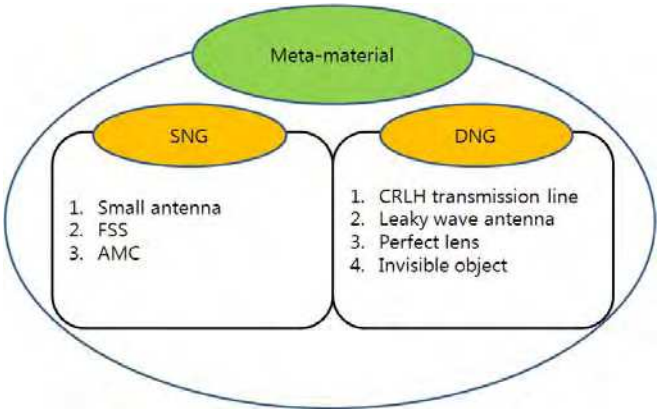

Fig. 2. The applications of meta-material concepts

3. NPLH transmission line

3.1 Introduction

Synthesis of meta-material structures has been investigated using various approaches. Amongst these approaches, the transmission line approach has been used to verify backward wave characteristics of LH transmission lines.

The pure LH (PLH) transmission line can be realized by a unit cell, which is composed of a series capacitor and a parallel inductor and must satisfy effectively homogeneous conditions. However it is difficult to realize an ideal pure LH transmission line, due to generation of parasitic RH (Right Handed) element characteristics of the transmission line which consist of a series inductor and parallel capacitor. A composite Right/ Left Handed (CRLH) transmission line structure concept is therefore used.

A balanced CRLH transmission line structure shows band pass characteristics. The LH dispersion range is below center frequency of pass band and the RH dispersion range is above the center frequency. The LH range is however typically narrow because it is limited by RH parasitic elements.

In this section we use a planar parallel plate structure to realise a NPLH transmission line with reduced RH element characteristics. Radiation loss calculations of the LH range is provided and the structure is optimized using CST MWS.

3.2 Analysis of transmission line

The CRLH transmission line and the unit cell of LH transmission line are shown in Fig. 3. The realization of LH transmission line based on microstrip line can't avoid parasitic RH components such as C'_R andL'_R. However, if the C_R and L_R approximate open state and short state, The Pure LH line can be realized. Consequently, in this paragraph, we replace ground plates as ground lines to reduce C'_R . Also, the signal line is composed by contiuous capacitive plates for minimization ofL'_R.

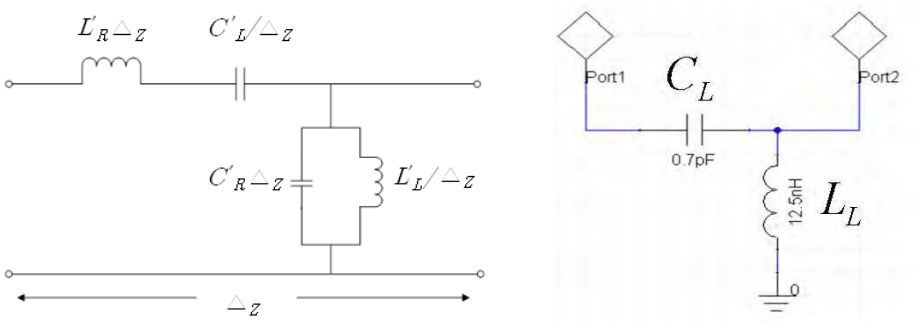

(a) CRLH transmission line (b) PLH transmission line circuit

Fig. 3. The CRLH transmission line and the unit cell of LH transmission line

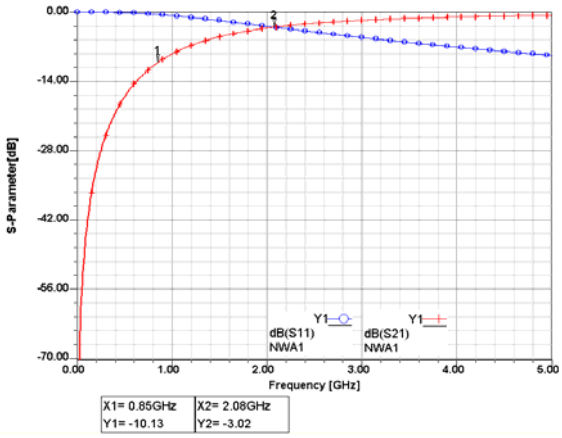

Fig. 4. The S-parameter of PLH transmission line circuit

The PLH transmission line circuit is shown in Fig. 3(b). A large series capacitance of PLH transmission line is needed for applying matched condition in low frequency band, but it is difficult to realize C_L because it needs very large dimesion. To reduce of physical size of PLH transmission line, the equivalent circuit of proposed transmission line is provided in unmatched conditin. The S-parameter of PLH transmission line circuit is shown in Fig. 4. The cutoff freqency(ω_{CLH}) of PLH transmission line has equation as following

$$\omega_{CLH} = 0.5\frac{1}{\sqrt{C_L L_L}} \tag{3}$$

The ω_{CLH} is about 850MHz. The pass band starts at 2.08GHz. The equivalent circuit of 2 cell-NPLH characteristic is shown in Fig. 5. Near the port 2, the C_R is added in order to achieve the reciprocal characteristic between 1-port and 2-port. Most CRLH transmission line has a weak point in analysis using circuit simulation. Specially, the important factors of PLH transmission line are phase and radiation loss. The additional components, which are generated by coaxial probe, must be considered for analysis of phase in PLH transmission line. The coaxial feed section, which consists of C_f and L_f, is added at equivalent circuit of 2 cells-PLH transmission line.

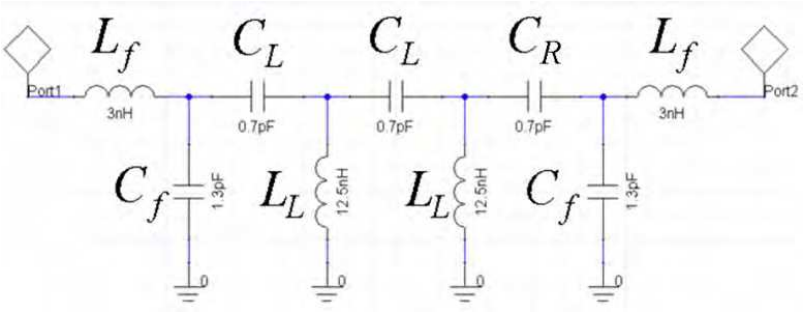

Fig. 5. The equivalent circuit of 2-cells NPLH transmission line

When the coaxial feed section is applied at equivalent circuit, two differences are shown. First is a change of pass band range and second is a srtart point of phase.
The S-parameter of NPLH transmission line equivalent circuit is shown in Fig. 6. The cutoff frequency is 0.92GHz. The resonance frequencies are 1GHz and 2.05GHz. The transmission bandwidth (over -3dB)of the transmission coefficient is 1.08GHz.
The loci of transmission coefficient of equivalent circuit are shown in Fig. 7. It is important result to realize NPLH transmission line physically, the phases of NPLH transmission line must coincide with the phases of equivalent circuit each frequency.

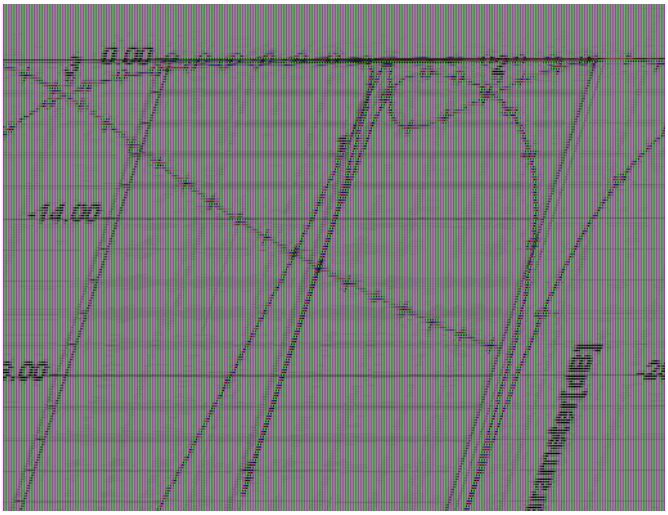

Fig. 6. The S-parameter of NPLH transmission line equivalent circuit

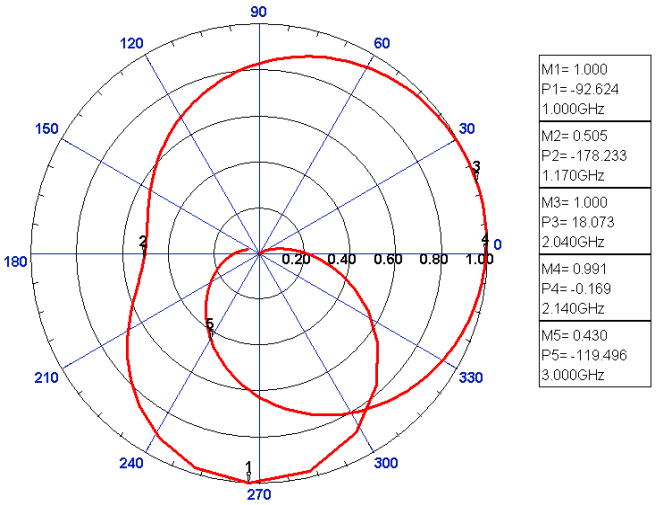

Fig. 7. The loci of transmission coefficient at equivalent circuit

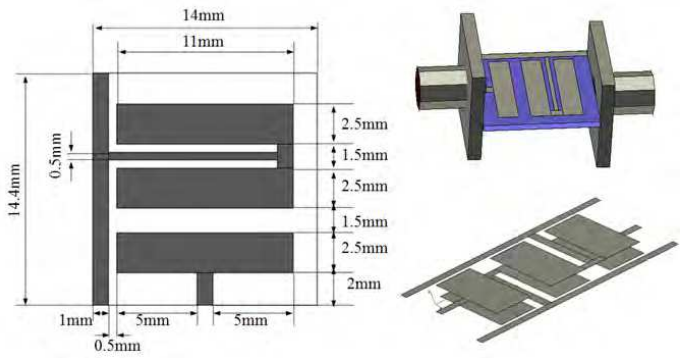

Fig. 8. The geometry of proposed NPLH transmission line

3.3 Simulated and experimental results

The geometry of proposed NPLH transmission line is shown in Fig. 8. The proposed NPLH transmission line consists of MIM (Metal-Insulate-Metal) capacitor and parallel inductor line. The physical size of componetns is calculated by distributed elements design.

The ground plane of proposed NPLH transmission line is simplified as line structure for reduction of parallel capacitor between ground and signal line. Also, to reduce series inductance, the transition line among cells is very short length. The substrate of proposed NPLH transmission line is Teflon, which is relative permittivity constant is 2.17. The S-parameter using 3D filed simulation is shown in Fig. 9. There is similarity between S-parameter results of 3D field simlation and equivalent circuit. The resonance frequencies are 1.17GHz and 2.15GHz. The pass bandwidth (over -3dB) of transmission coefficient is 0.94GHz. Also loci of transmission coefficients between equivalent circuit and 3D field simulation are very similar. The loci of transmission coefficent using 3D filed simulation are shown in Fig. 10. The proposed NPLH transmission line achieves near pure left handed characteristic.

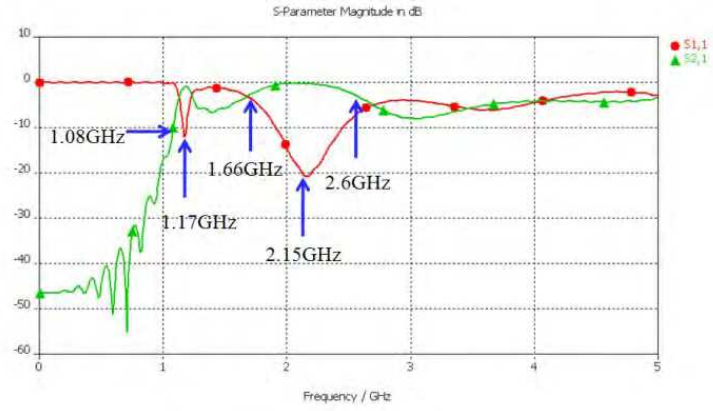

Fig. 9. The S-parameter using 3D filed simulation

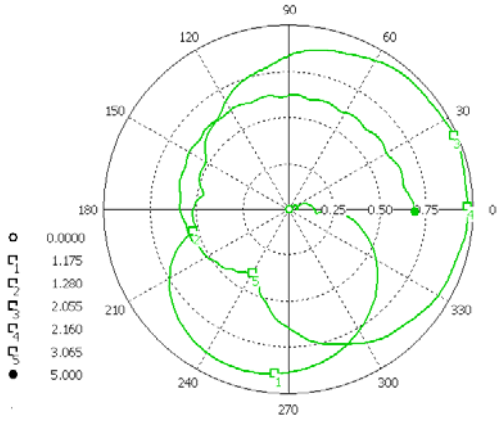

Fig. 10. The loci of transmission coefficent using 3D filed simulation

The backward wave characteristic is shown at frequency range below 3GHz. Due to limitation of a distributed elements design at frequency range over 3GHz The normal E-field distrigution at 2.15GHz is shon in Fig. 11.
The insertion loss is related with a radiation loss. In case of proposed NPLH transmission line, if the total power is 100%, the transmission power is calculated as following two equations.

$$S_{21r}[\%] = 100 - 100 * 10^{S_{11}[dB]/10}, \qquad S_{21i}[\%] = 100 - 100 * 10^{S_{21}[dB]/10} \tag{4}$$

Where, S_{21r} and S_{21i} are calculated at reflection coefficient and insertion loss respectively. The radiation power(P_{rad})is expected as following equation

$$P_{rad}[\%] = S_{21r}[\%] - S_{21i}[\%] \tag{5}$$

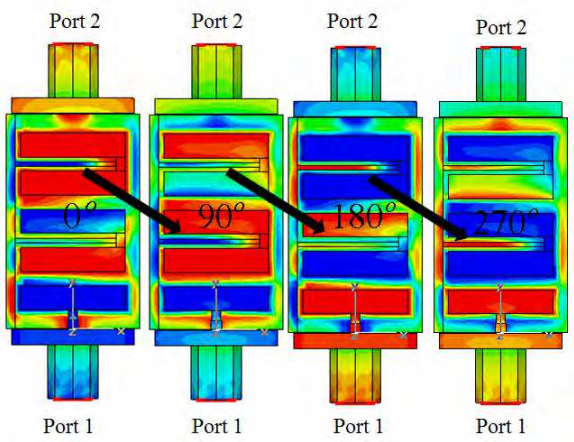

Fig. 11. The normal E-field distribution at 2.15GHz

The P_{rad}, which is calculated at 2.6GHz, is about 33%. There are very similar results between P_{rad}[%] and radiation efficiency of 3D simulation result. The radiation losses at each frequencies are shown in Table1.
The photo and measured S-parameter of fabricated NPLH transmission line is shown in Fig. 12. The pass bandwidth of transmission coefficient(over=3dB) is 1.78GHz.
The NPLH transmission line using prallel plate structure is proposed. The proposed structure shows backward wave characteristics which a PLH transmission line should have. The provided equivalent circuit model of a NPLH transmission line simulation results are similar with and ideal PLH transmission line characteristics. Also, The radiation loss which is deliverated by S_{11} and S_{21}. We understand realization method of near pure left handed transmission line using distributed elements and means of meta-material concepts in paragraph. We will study compact antenna using metamaterial concepts in next paragraph.

Frequency(GHz)	Radiation loss(%)	Frequency(GHz)	Radiation loss(%)
1.7	0.21	2.2	6.18
1.8	0.43	2.3	10.73
1.9	0.96	2.4	17.16
2	1.82	2.5	24.53
2.1	3.39	2.6	31.16

Table 1. Radiation losses of NPLH transmission line

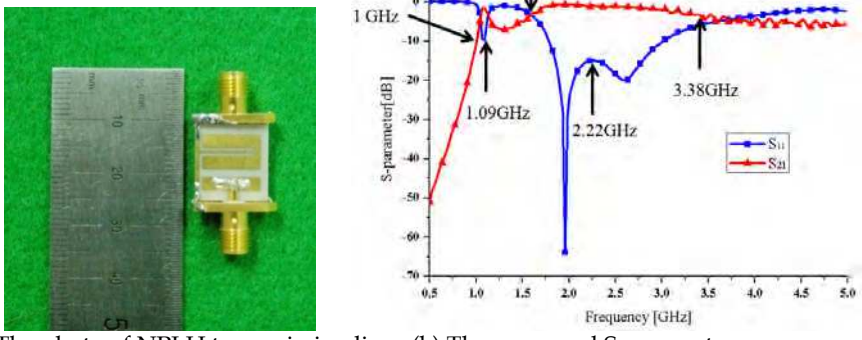

(a) The photo of NPLH transmission line (b) The measrued S-parameter
Fig. 12. The photo and measured S-parameter of NPLH transmission line

4. The compact antenna using meta-material concepts

4.1 Introduction

The electrically small antenna is defined as ka < 1 where k is the wave number and a is the maximum length of antenna. For electrically small antennas efficiency, gain, impedance bandwidth and quality factor (Q) vary as a function of maximum length of antenna. Miniaturization of an antenna typically results in narrower impedance bandwidth, higher Q and lower gain. The reduction of defects of small antennas is the main consideration in design of electrically small antennas.

Recently an EESA (Efficient Electrically Small Antenna) was proposed by Richard W.

Capacitance (unit: pF)		Inductance (unit: nH)		Resistance (unit: Ω)			
C_f	1.2	L_m	4	R_1	40.7k	R_2	0.637
C_m	0.15	L_g	36	R_3	81k	R_4	0.779

Table 2. The values of equivalent circuit elements

Ziolkowski in 2006 and simulated using HFSS. The EESA was achieved using a spherical shell of SNG (Single Negative) or DNG (Double Negative) materials. The SNG and DNG material characteristics are realized using electrical structures. These techniques will be applied for miniaturization of an antenna in this section.

4.2 The equivalent circuit of small antenna using ENG material concepts

The concept of proposed antenna is shown in Fig. 13. The equivalent circuit of proposed small antenna is shown in Fig. 14. Generally the small monopole antenna has a high capacitance due to very short length. Therefore the inductance loading is necessary for the impedance matching of a small monopole antenna. The impedance matching can be achieved by negative permittivity meta-material structure, which is equivalent parallel inductance in this paragraph.

The two port equivalent circuit of proposed antenna is realized by open condition. The C_f is a capacitance of coaxial feed and feeding pad. The L_m is an inductance of monopole antenna and coaxial feed. The C_m is a capacitance among monopole antenna, ground and negative permittivity meta-material structure.

We find that parallel inductance is operated as negative permittivity in first paragraph. The L_g is an inductance of negative permittivity meta-material structure in effective material. The values of equivalent circuit elements are shown in table 2. The resonance frequency of equivalent circuit is 2.04GHz

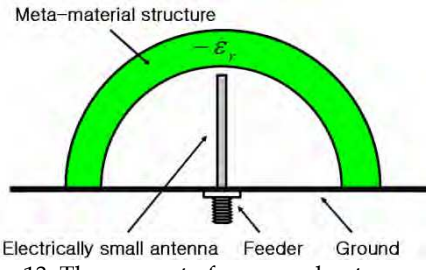

Fig. 13. The concept of proposed antenna

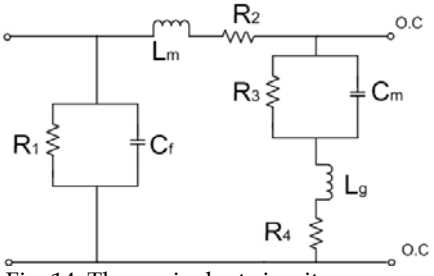

Fig. 14. The equivalent circuit

4.3 The realization and experiment of small antenna using equivalent circuit

The idea and geometry of the proposed antenna are shown in Fig 15. The substrate is FR4 (ε_r: 4.9) and the substreate thickness is 0.8mm. The proposed antenna is excited by a coaxial feed structure. The geoemtry is obtained by calculated passive components.

We consider thin wire in free space. The length of thin wire is about 0.5 λ for resonance condition. The resonated thin wire has high inductive characteristic at lower band of

resonance frequency. This factor can be applied for negative permittivity in proposed structure. But we have to reduce length of thin wire and apply shorted thin wire for small antenna. The shorted thin wire is alternated as defected ground structure, which is called meta-material structure in this geometry. The inductance of coaxial feed and monopole are insufficiency for resonance of antenna. Therefore, the additional inductance is needed and realized by meta-material structure.

The simulated characteristics of proposed antenna are shown in Fig. 16. The resonance frequency and the impedance bandwidth (VSRW ≤ 2) are 2.035GHz and 155MHz at 3D field simulated results. We find that loci of impedance are very similar between circuit simulation and 3D filed simulation. The geometry is corresponded with equivalent circuit. The field distribution of proposed antenna is shown in Fig. 17(a). The normal E-field is concentrated between monopole and negative permittivity meta-material structure.

We see that surface currents are flowed on negative permittivity meta-material structure in Fig. 17(b). Therefore the negative permittivity meta-material structure is operated as inductance L_m in equivalent circuit. The negative permittivity meta-material structure is used for impedance matching and high performance of small monopole antenna.

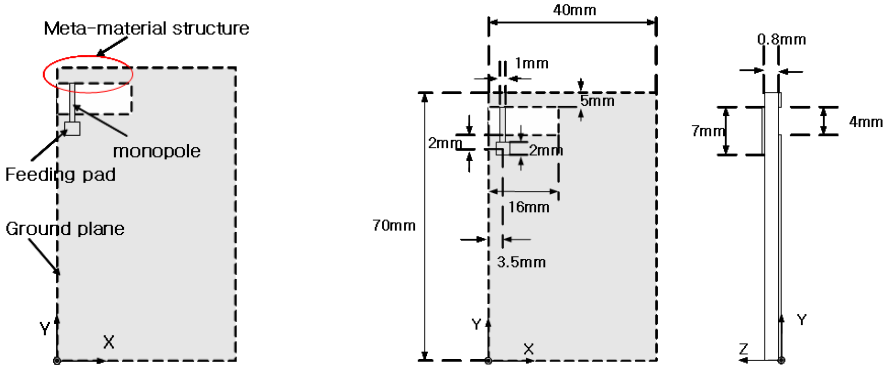

(a) The idea of proposed antenna (b) The geometry of proposed antenna

Fig. 15. The concept and geometry of proposed antenna

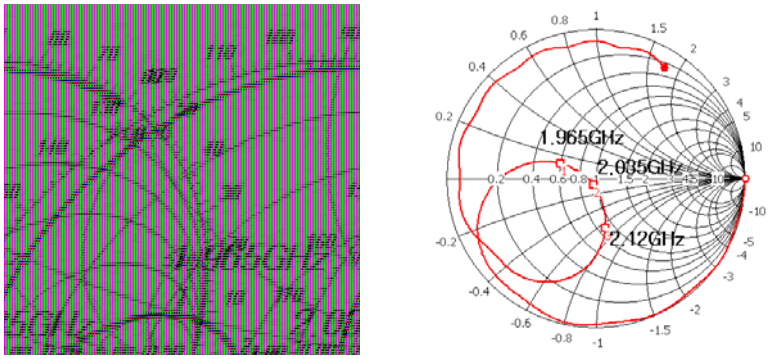

(a) Circuit simulation (b) 3-dimensional field simulation

Fig. 16. The loci of input impedance on a smith chart for circuit simulation and 3D field simulation

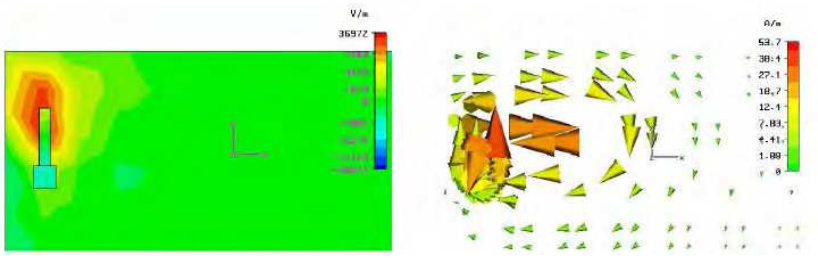

(a) Normal E-field (b) Surface currents

Fig. 17. The field distribution of proposed antenna

The photo of fabricated antenna is shown in Fig. 18(a). The measured return loss is shown in Fig. 18(b). The resonance frequency is 2.04GHz. The measured impedance bandwidth (VSRW ≤ 2) is 174MHz.

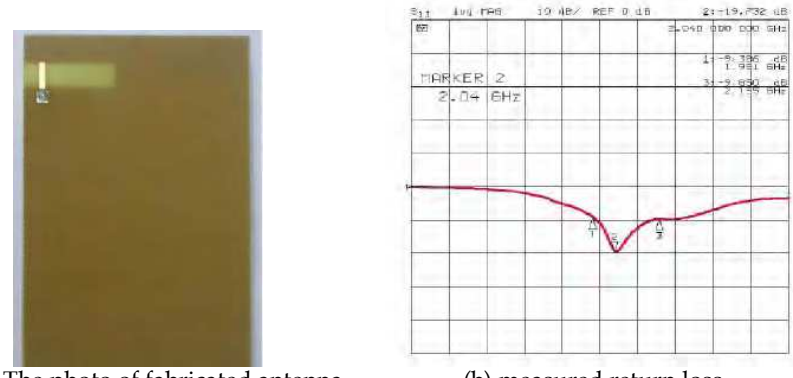

(a) The photo of fabricated antenna (b) measured return loss

Fig. 18. The photo and measured return loss for proposed antenna

The inner cylinder of coaxial probe and monopole are dominant section of radiation pattern. Therefore, the omni directional pattern is achieved. The values of efficiencies and maximum gains are shown in Table 3. The maximum gain and efficiency are 3.6dBi and 77.8% respectively at the frequency of 2.1GHz. We calculate theoretical quality factor(Q_L), which is 108, using maximum length of monopole and measured quailty factor (Q_m), which is 7.21, using fractional bandwidth. We find that the quality factor is lowered by negative permittivity meta-material structure and the improvement of small antenna can be achieved by meta-material concepts.

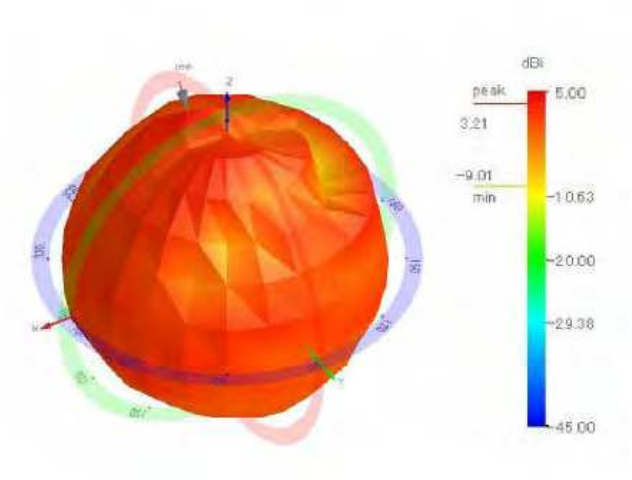

Fig. 19. The measured radiation pattern of fabricated antenna

Frequency [MHz]	Maximum gain [dBi]	Efficiency
1900	2.036	49.97%
2000	2.982	72.36%
2040	2.986	73.64%
2100	3.603	77.76%
2200	2.487	64.89%
2300	2.128	53.50%

Table 3. The values of efficiencies and maximum gains

5. Directive radiation of electromagnetic wave using dual-band artificial magnetic conductor structure

5.1 Introduction

In this paragraph, the FSS and AMC structures can be analyzed by a view point of effective medium. So we will find means of FSS and AMC using new analysis method, which will be proposed using periodic boundary condition. The verified FSS and AMC structure will be applied to enhance directivity of antenna. The enhancement of directivity of antenna will be achieved by febry perot resonance condition between FSS and AMC structure.

5.2 The enhancement of directivity using FSS structure

The meta-materials concept can be realized by electrical structures, which adjust refractive index of material. So we can achieve enhancement of directivity using FSS structure, which is analyzed in negative permittivity of effective medium.

The febry perot interferometer is shown in Fig. 20. The source generates wave power ($P_i \cos\theta$), which propagates to medium 2 and is reflected. The reflected wave power is

propagated to medium 1 and reflected by medium 1. The generated and reflected wave powers are combined. The reflected wave power (P_r) and total power (P_t) of generated and reflected wave are expressed by equation (6) and equation (7) briefly.

$$P_r = P_i \cos\left(2\frac{2\pi}{\lambda}\cdot d + \phi_1 + \phi_2 + \theta\right) \tag{6}$$

$$P_t = P_i \cos\theta + P_r \tag{7}$$

Where, the d, ϕ_1, ϕ_2 and θ are distance, phase variation at medium 1, shifted phase at medium 2 and initial phase respectively. These equations didn't consider radiation loss and additional reflected wave.

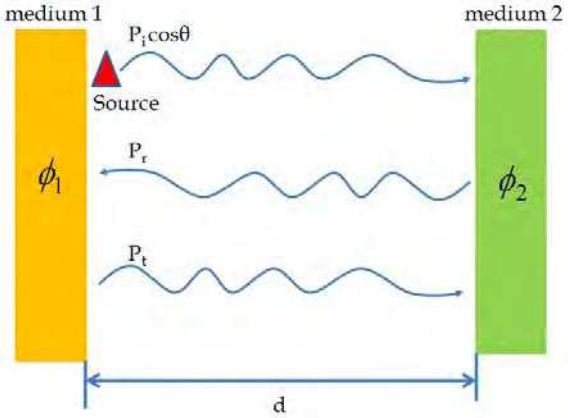

Fig. 20. The febry perot interferometer

If the medium 1 and medium 2 are perfect electric conductor, the shifted phase (ϕ_1, ϕ_2) of medium is 180 degree. Therefore, if the distance is λ/2 between medium 1 and medium 2, the total power is maxed.
The enhancement of directivity can be achieved by FSS structure. The source, medium 1 and medium 2 are replaced with antenna, ground and FSS structure. The optimized distance is about λ/2 between ground and FSS structure. If the periodic spaces between lattices are very short below one wave length.
The FSS can be analyzed at a point view of effective medium. The equivalent effective permittivity (ϵ_{eff}) of FSS structure is expressed by equation (8).

$$\epsilon_{eff} = 1 - \omega_p^2/\omega^2 \tag{8}$$

Where, the ω_p is plasma angular frequency, the ω is availabe angular frequency.

The effective permittivity is negative below plasma angular frequency, however the effective permittivity of FSS structure is near 0 over plasma angular frequency. This characteristic is applicable for enhancement of directivity. The concept of lens using FSS structure is shown in Fig. 21.

But this method has pebry ferot resonance distance, which is $\lambda/2$, between FSS strucuture and antenna. The physical height is very large in antenna using FSS structure. If we can adjust shifted phase of ground plane in antenna, we can reduce distance between FSS structure and antenna. So we will find AMC for miniaturization of distance in next paragraph.

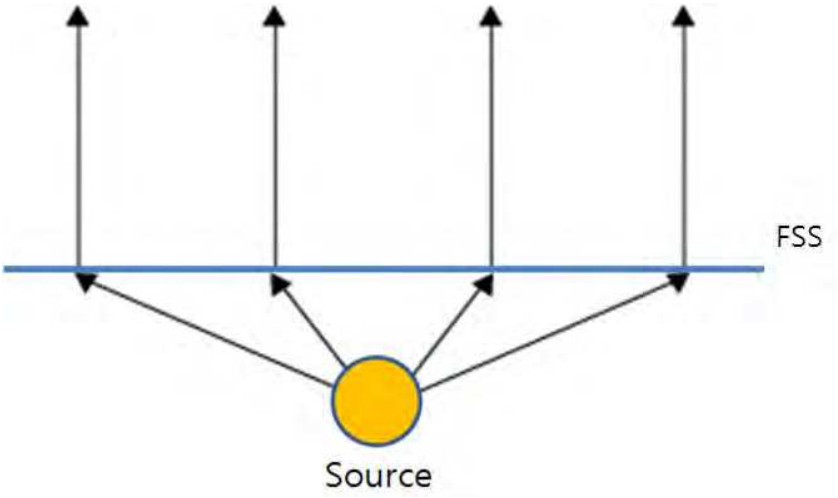

Fig. 21. The concept of lens using FSS strucuture

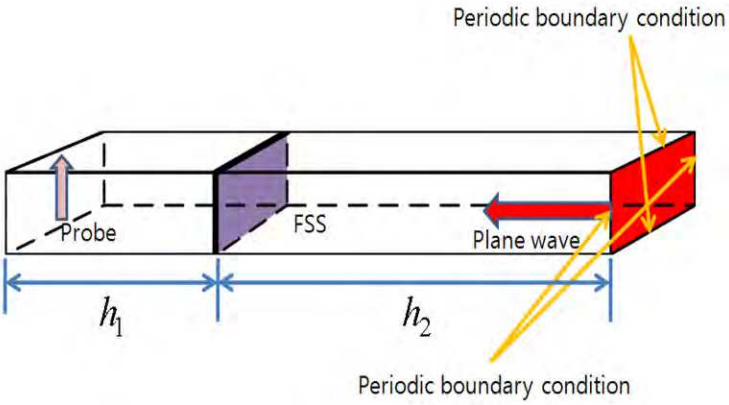

Fig. 22. The analysis method for FSS

5.3 The enhancement of directivity using FSS structure

In this paragraph, we propose analysis method for FSS, which is expressed by Fig. 22.
The incident plane wave is propagated to unit cell of FSS. The space (h_2) between unit cell of FSS and plane wave source is λ_0. The space (h_1) between FSS and probe is $\lambda_0/4$. These are enclosed by periodic boundary condition.

We think that the plane wave, unit cell of FSS and probe are alternated with signal, FSS plate and receiving antenna. So if the electric filed of received signal is maxed, the unit cell of FSS is operated as FSS lens. The unit cell of FSS structure is shown in Fig. 23. The unit cell is designed using square ring slit on substrate. The substrate is Reogers RO3210, the thickness and relative permittivity are 1.27mm and 10.2 respectively. The unit cell of FSS is alternated with infinite FSS plate using periodic boundary condition.

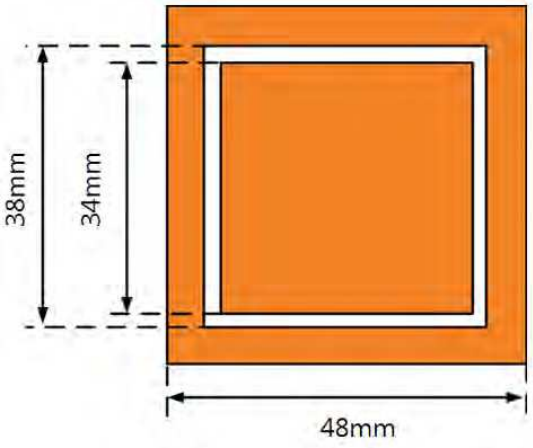

Fig. 23. The unit cell of FSS structure

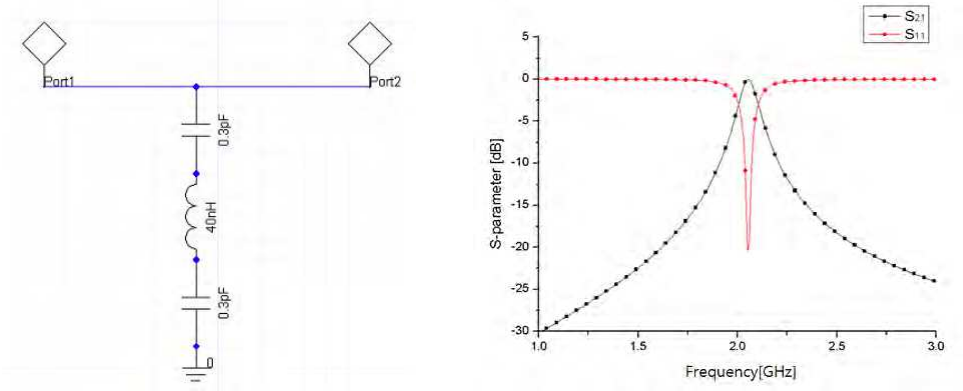

(a) Equivalent circuit of unit cell (b) The S-parameter of unit cell

Fig. 24. The unit cell of FSS structure

We think that the infinite conductor plate with periodic square ring slits. If the conductor plate with periodic square ring slits is excited by plan wave, the difference voltage between inner conductor and outer conductor is generated by square slits and the currents are induced along conductor. Therefore, the capacitance is generated between inner conductor and outer conductor.

The inductance is provided by induced currents. The equivalent circuit and S-parameter of unit cell is shown in Fig. 24. The generated capacitance and inductance are 0.3pF and 40nH.

The received E-filed is shown in Fig. 25(a). It is maximum E-field at 2GHz. The fractional band width is 950MHz (1.6GHz~2.55GHz). The phase of received signal is expressed in Fig. 25(b). The phase of received signal is 90º at 2GHz.

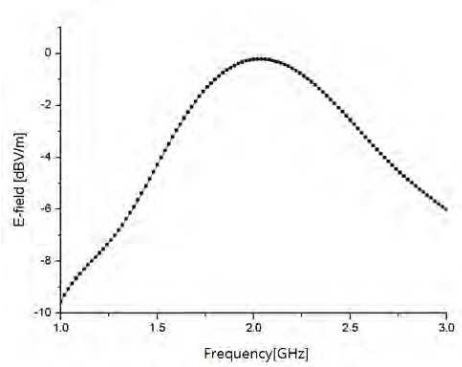

(a) Received E-field

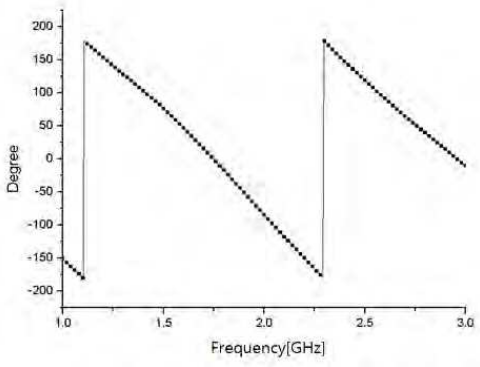

(b) Phase of received signal

Fig. 25. The unit cell of FSS structure

5.3 The enhancement of directivity using AMC structure

In this paragraph, we find mean of AMC and propose the dual band AMC structure, because the defect of AMC technology is narrow operation bandwidth.

We suppose that the vertical plane wave is propagated to boundary between medium 1 and medium 2. The incident plan wave at boundary between medium 1 and medium 2 is shown in Fig. 26. The Electromagnetic field of incident plane wave can be expressed by equation (9)

$$\overrightarrow{E_i}(z) = \overrightarrow{a_x} E_{i0} e_1^{-j\beta_1 z}, \qquad \overrightarrow{H_i}(z) = \overrightarrow{a_y} \frac{E_{i0}}{\eta_1} e_1^{-j\beta_1 z} \tag{9}$$

Where, the E_{i0}, β_1 and η_1 are magnitude, phase constant and wave impedance at medium 1. The incident plane wave is divided by discontinuous mediums. A part of incident plane wave is transmitted continuously in medium 2. The rest part is reflected at boundary. The reflected plane wave is expressed by fallowing equation.

$$\overrightarrow{E_r}(z) = \overrightarrow{a_x} E_{r0} e^{j\beta_1 z}, \qquad \overrightarrow{H_r}(z) = -\overrightarrow{a_z} \times \frac{1}{\eta_1} \overrightarrow{E_r}(z) = -\overrightarrow{a_y} \frac{E_{r0}}{\eta_1} e^{j\beta_1 z} \tag{10}$$

The transmitted plane wave is expressed by fallowing equation

$$\overrightarrow{E_t}(z) = \overrightarrow{a_x} E_{t0} e^{-j\beta_2 z}, \qquad \overrightarrow{H_t}(z) = \overrightarrow{a_z} \times \frac{1}{\eta_2} \overrightarrow{E_t}(z) = \overrightarrow{a_y} \frac{E_{t0}}{\eta_2} e^{-j\beta_2 z} \tag{11}$$

Where, E_{t0}, β_2 and η_2 are magnitude, phase constant and wave impedance respectively at z=0.

The relation of electric fields and magnetic fields can be expressed by equation (12)

$$\overrightarrow{E_i}(0) + \overrightarrow{E_r}(0) = \overrightarrow{E_t}(0), \qquad \overrightarrow{H_i}(0) + \overrightarrow{H_r}(0) = \overrightarrow{H_t}(0) \tag{12}$$

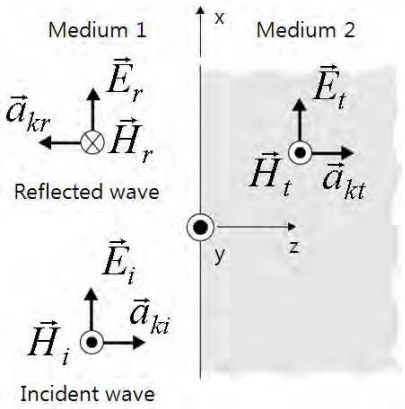

Fig. 26. The incident plan wave at boundary between medium 1 and medium 2

The magnetic field can be replaced with electric field using wave impedance and expressed by equation (13)

$$\frac{1}{\eta_1}(E_{i0} - E_{r0}) = \frac{E_{t0}}{\eta_2} \tag{13}$$

The reflection and transmission electric fields are expressed by equation (14) using equation (12) and (13).

$$E_{r0} = \frac{\eta_2 - \eta_1}{\eta_2 + \eta_1} E_{i0}, \qquad E_{t0} = \frac{2\eta_2}{\eta_2 + \eta_1} E_{i0} \tag{14}$$

The reflection and transmission coefficient can be extracted using equation (14). The reflection and transmission coefficients are fallowing equation (15).

$$\Gamma = \frac{E_{r0}}{E_{i0}} = \frac{\eta_2 - \eta_1}{\eta_2 + \eta_1}, \qquad \tau = \frac{E_{t0}}{E_{i0}} = \frac{2\eta_2}{\eta_2 + \eta_1} \tag{15}$$

We see the reflection coefficient. If medium 2 is conductor, the wave impedance (η_2) is 0. So reflection coefficient is -1. But if medium 2 has very high impedance like as infinity impedance, the reflection coefficient is 1. Therefore, the mean of AMC is electrical structure for infinity wave impedance. The wave impedance (η_2) is fallowing equation (16)

$$\eta_2 = \sqrt{\frac{\mu_2}{\epsilon_2}} \tag{16}$$

Finally, the AMC can be achieved by near zero permittivity or infinity high permeability. How can we achieve AMC structure? The realization of AMC can be found using resonance structure. The representative AMC structure, which is mushroom structure and equivalent circuit are shown in Fig 27.